Available online at www.sciencedirect.com
SCIENCE DIRECT®
Journal of Power Sources 116 (2003) 193–202
JOURNAL OF POWER SOURCES
www.elsevier.com/locate/jpowsour

A study of current and potential distributions on tubular positive plate

Yonglang Guo*, Weizhen Li, Le Zhao

Department of Chemistry, Shandong University, Jinan 250100, PR China

Abstract

The distributions of current and potential on the tubular positive plate have been studied by measuring the IR drop in the H_2SO_4 solution between the positive and negative plates. It is found that lower polarization and higher current appear in the upper part of the plate. But the resistance of the active mass develops very rapidly at the top and at the bottom of the plate. This leads to very high polarization and low current in these regions in the later stage of the discharge. And it is interesting to find that the potential difference up and down the plate is mainly caused by the interface resistance between the active mass and the spine.

Keywords: Distributions of current and potential; Lead-acid batteries; Tubular positive plate

1. Introduction

The tubular positive plate of lead-acid batteries has been widely studied over the decades. The investigations mainly concentrate on its manufacture [1–6], its formation [7–10] and the grid or current collector design [11–15], etc. The swelling and shedding of the positive active mass are essential to limiting the life of lead-acid batteries in the cyclic application. Since the gauntlets of the tubular positive plates provide good resistance to expansive forces of active mass, the shedding is prevented and the battery has a very good performance in the cyclic applications. Therefore, up to now, the majority of motive-power cells and stationary batteries for industrial applications, especially large cells, still use the tubular positive plate design, to ensure their high reliability, long life and total capacity output.

The majority of tubular positive plates are used to produce the large lead-acid cell. Most of the plates are about 30–160 cm high. In this case, the great voltage drop of the plates from the top to the bottom appears at a high discharge rate, so that the current and potential distributions on the plate surface and the active mass utilization ratio become nonuniform. A lot of optimized designs and simulations have been developed for the tubular positive plates and the conventional orthogonal grids of the automotive batteries [11,12,16–19]. Sunu and Burrows [16] and Vaaler et al. [17] predicted the potential and current distributions on the surface of the orthogonal grids, according to each intersection and the conductivity of grid members. Calabek [18,19] simulated the discharge of a positive–negative electrode pair and optimized the orthogonal grid design according to the current distribution. With the aid of a computer, Asai et al. [11] calculated the changes in the current and potential distributions on the surface of the tall tubular positive plate according to the plate resistance and the current–potential–time relationship. Various current-collector designs at the top, middle and bottom significantly improved the discharge performance of the tubular positive plates.

The aim of this paper is to measure the current and potential distributions of the actual tubular positive plate so as to further understand the active mass utilization, the voltage drop up and down the plate, the change in the resistance and the factors influencing the discharge performance of the cell.

2. Experimental

The tubular positive plate tested consisted of 15 dacron tubes with internal diameter of 0.85 cm and current collectors with the spine diameter of 0.3 cm. The lead spine was Pb-5%Sb alloy. The plate had a dimension of 13.5 cm × 34.5 cm and is shown in Fig. 1. 840 g dry powder of ball-mill oxide was filled and the average filling density was 3.4 g cm^{-3}. After curing and drying, tank formation of the positive plate was

* Corresponding author.
E-mail address: yguo@sdu.edu.cn (Y. Guo).

0378-7753/03/$ – see front matter
doi:10.1016/S0378-7753(02)00691-2

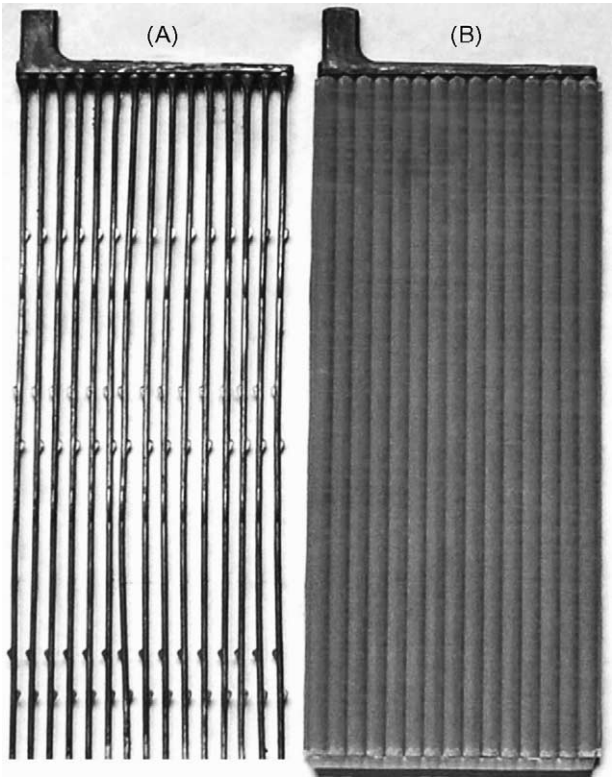

Fig. 1. Pictures of the tubular positive plate and its spine.

performed in 1.05 specific gravity H_2SO_4 in the range of 30–45 °C. The formation input was about 600 Ah per kg oxide in 45 h.

The initial charge amount of the tubular positive plate was 216 Ah in 1.285 specific gravity H_2SO_4 in 70 h. In charge–discharge, the tubular positive plate was put between two negative plates. The distance between the positive and negative plates was about 4.5 cm. The width of the container and the height of the H_2SO_4 electrolyte were the same as the dimensions of the tubular positive plate, to ensure the ion flowing between negative and positive plates, which were parallel to each other. Since an IR voltage drop could appear in the H_2SO_4 electrolyte between the plates during discharge, a couple of reference electrodes with 3 cm in between, perpendicular to the plate, were used to measure the voltage drop in the electrolyte so as to know the current density on the tubular positive plate surface. The spacing of three $Hg/Hg_2SO_4/H_2SO_4$ (1.285 specific gravity) reference electrodes was 2.5 cm. The outside diameter of the reference electrode tip was about 0.15–0.2 cm. When three couples of reference electrodes were moved from the bottom to the top twice, we could get the current and potential distributions of six channels on the entire tubular positive plate surface. The voltage drop between the reference electrodes and the electrode potentials of the plate were recorded by a HP 34970A Data Acquisition/Switch Unit connected to a PC computer. The experiments were conducted at room temperature (23 ± 2 °C).

3. Results and discussion

3.1. Distributions of current density and potential

When the tubular positive potential was discharged at 50 A (1 h rate), a big IR drop appeared in the H_2SO_4 solution between the positive and negative plates, which could be measured by a couple of reference electrodes. Since the top of the tubular positive plate was a horizontal current collector and the bottom was a bar of plastic seal, there was no active mass on the top and at the bottom, 1.2 cm of each, respectively. So the IR drop of six channels with equi-interval was measured only from the bottom to the top of the active mass in the gauntlets. The filling oxide was 32 cm in height. In this case, 390 data of the potential difference were recorded when the measurements were carried out every 0.5 cm. Since the IR drop is proportional to the ion flow or current in the solution, the current density on the plate can be calculated on the basis of the discharge current, the area of the plate and each IR drop in the solution. Fig. 2 shows the distribution of current density at the very beginning and the end of discharge, respectively. It is found that the current density rises gradually with the increase in height on the plate. In Fig. 2A, a low current density appears on the top and at the bottom of the plate. This is because some ions around the plastic bar seal and the current collector on the top can not move in a parallel way from this plate to another. At the end of the discharge in Fig. 2B, the current density on the top and at the bottom decreases obviously. Fig. 3 shows the evolution of the current density distribution in one of the channels during the discharge. It can be seen that the current density on the top of the plate drops quickly during the discharge. It is clear that the active mass on the top is easier to discharge than that on the other parts in the early stage of the discharge. And the overcharge and overdischarge always occur on the top of the plate so that the resistance of this part of active mass becomes high in the cyclic application. The low current at the bottom may be related to the low filling density of the oxide and the interface resistance between the lead spine and the active mass (this will be discussed below). Since the discharge current is unchanged, the current density in the middle of the plate increases with the decrease of the current density at the top during the discharge. It can also be seen that the measured current density tends to rise when the reference electrodes elevate along the plate, except at the top and at the bottom 4–5 cm of the plate.

When the positive plate is discharged, the H_2SO_4 in the solution must diffuse to the surface of the active mass and react with PbO_2 to form $PbSO_4$. At this time, a concentration gradient of H_2SO_4 appears in the solution near the surface of the plate so that the positive potential drops quickly in the initial period of the discharge. But the change of potential caused by the concentration difference tends to stabilize when the tubular positive plate is discharged at 50 A (1 h rate) for 2 min. Fig. 4 shows the distribution of the positive potential at the beginning and the end of the discharge,

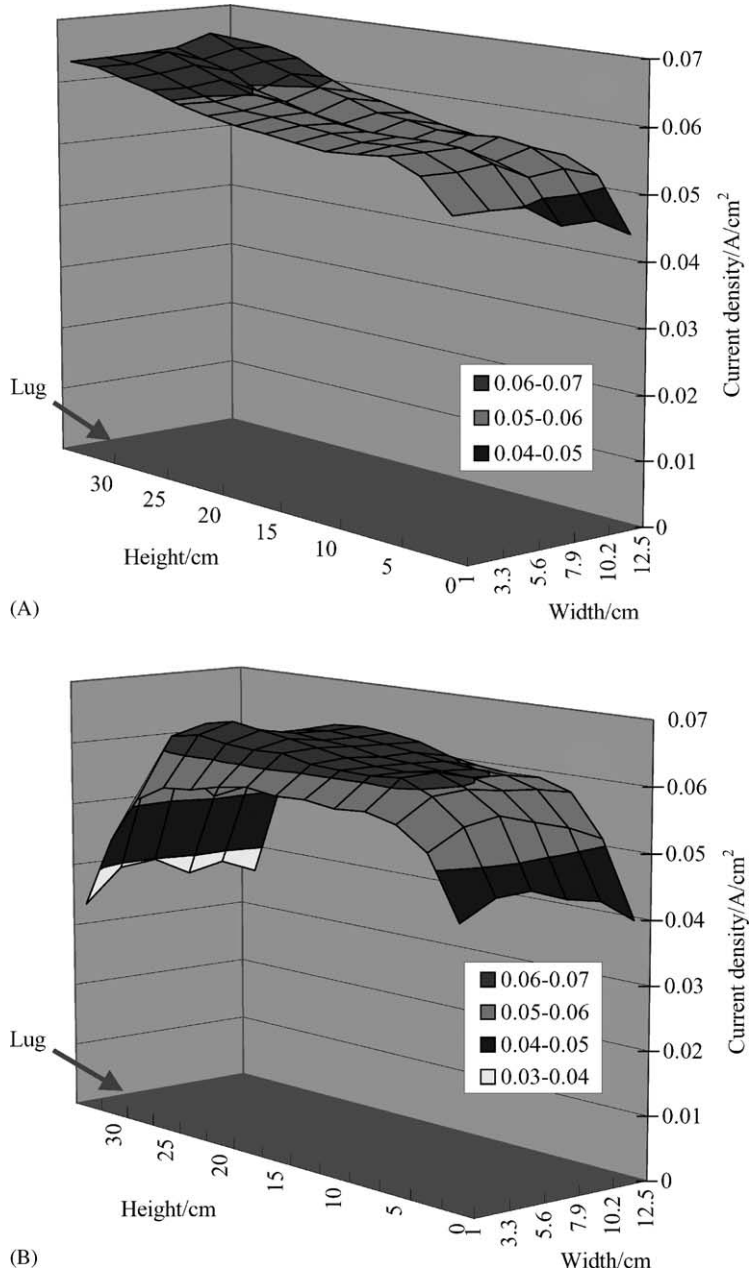

Fig. 2. The distribution of current density on tubular positive plate during discharge of 50 A (1 h rate). Discharge time: (A) 0 min; (B) 60 min.

respectively. Since the positive potential drops steadily during the discharge, there appears a difference between the positive potentials in both measurements in Fig. 4. From Fig. 4A, we can see that the positive potentials increase linearly from the bottom to the top of the plate. But Fig. 4B shows that a great change takes place in the potential distribution at the end of the discharge, especially on the top and at the bottom. Fig. 5 shows the changes in the distribution of the positive potential in one of the channels during the discharge. It is found that the potential difference up and down the plate exceed 100 mV during the discharge of 50 A. And the positive polarization increases almost constantly with the discharge of the tubular positive plate. But the positive overpotential increases more quickly at the top and at the bottom. In comparison with the change of the current density in Fig. 3, it shows that the resistance of the active mass becomes very high in these regions, especially at the top of the plate.

3.2. Utilization of active mass

The utilization of active mass is related to the design, manufacture and the height of the plate, etc. Generally speaking, the higher is the plate, the lower the utilization of the active mass at the bottom of the cell is. In our experiments, we measure the utilization of active mass at

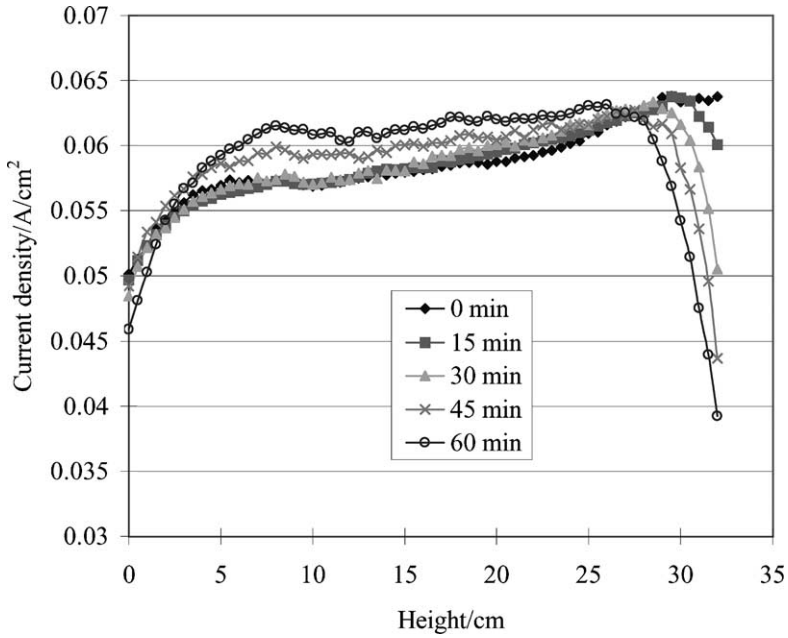

Fig. 3. The current density vs. height on the tubular positive plate in channel 2 (near lug) during discharge of 50 A (1 h rate).

different heights on the tubular positive plate. Since the current density of about 4–5 cm of the top and the bottom of the plate fall very quickly in Fig. 3 because of the change in the resistance, the points at the heights of 5, 17.5 and 30 cm were chosen. We fixed three couples of reference electrodes at these height points in the direction perpendicular to the plate. According to the data of the IR voltage drop obtained, the current density can be calculated and its evolution is shown in Fig. 6. It is seen that the current density in the upper part of the plate is higher than that in the lower part before 85% degree of discharge (DoD). During discharge, the current density in the upper part falls while that in the middle and lower parts increases. At the end of discharge, the change speeds up.

The filling of ball-mill oxide in the tubular positive plate was performed by a vibratory method. So the filling density was different up and down the plate. In order to measure the distribution of the filling density, we took out one tube from the filled plate and cut it into six parts. Each part is 5.4 cm long. Therefore, we can obtain the average filling density of each part according to the volume of the tube and the weight of spine and oxide. Fig. 7 shows the change in the filling density of ball-mill oxide in the tubular plate at different heights. It is observed that the filling density is almost unchanged in the middle, it decreases at the bottom of the plate and increases rapidly on the top. It is clear that this is caused by the vibration in the filling process.

The theoretical capacity of 840 g ball-mill oxide with 75% PbO is about 205.8 Ah. According to the current–time curves in Fig. 6, Fig. 8 shows the utilization ratio of the active mass at different heights on the tubular positive plate at discharge currents of 30 and 50 A, respectively. Although the current density in the upper part is higher than that in the middle, Fig. 7 shows denser and more oxide in the upper part so that the utilization of the active mass for these two parts in Fig. 8 is almost unchanged. This is because the greater height results in an increase of active mass utilization while the denser oxide leads to its decrease. In the lower part of the plate, the active mass utilization falls significantly. This is closely related to the low filling density and low electrochemical polarization. Therefore, it is believed that the utilization of the active mass is quite uneven on the tall tubular positive plate. It depends on the height of the plate, the discharge rate and the homogeneous filling density, etc.

3.3. The changes in resistance of the tubular positive plate

The resistance of a plate or cell is normally measured by interrupting the circuit [20]. In this case, the resistance at different parts of the plate can not be obtained. Of course, it is very difficult to get the resistance distribution on the plate. However, it is very important for us to understand the change in the resistance for a tall plate. The resistance in different regions on the plate can be defined as the ratio of the overpotential to the current density at this point. For the tubular positive plate in Fig. 1, the overpotential in any part, η, mainly consists of

$$\eta = \eta_e + \eta_{am} + \eta_c + \eta_{IR} + \eta_{interface} \quad (1)$$

where η_e denotes the polarization potential of the electrochemical reaction, η_{am} the polarization potential of the active mass, η_c the overpotential of the concentration difference, η_{IR} the voltage drop caused by the lead spine and $\eta_{interface}$ the voltage drop of the interface between the spine and the active mass.

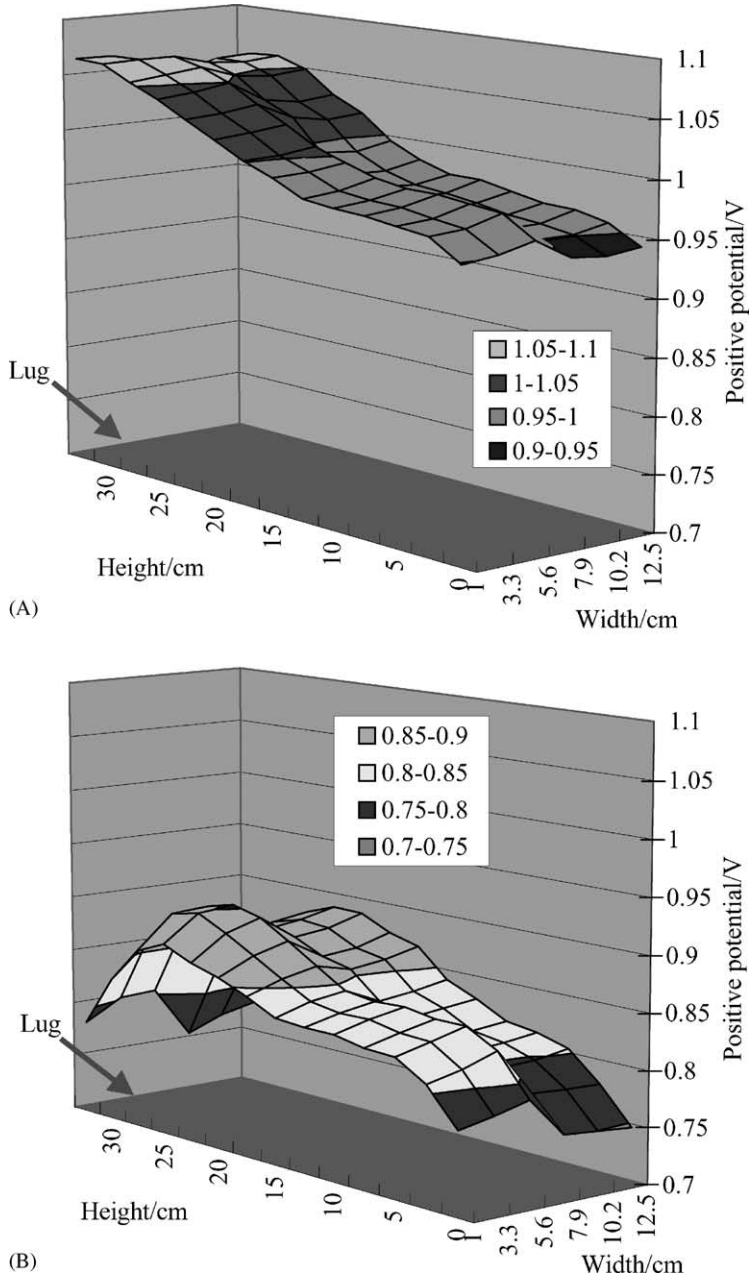

Fig. 4. The distribution of positive potential on the tubular positive plate during discharge of 50 A (1 h rate). Discharge time: (A) 2 min; (B) 60 min.

When a positive plate is fully charged, the resistance of the positive plate reaches a minimum. Then it increases and the positive potential decreases during the discharge. So the evolution of the resistance in the active mass can be obtained by measuring the changes in the potential and current, even though we do not know the actual resistance value. The positive potential falls very quickly at the beginning of the discharge because of the change in the H_2SO_4 concentration difference near the surface of the plate. In our experiments, the H_2SO_4 solution is excessive and its specific gravity only decreases by 0.008 g cm^{-3} in the entire discharge of 50 A. Therefore, it is reasonable to assume that the H_2SO_4 concentration and its concentration difference near the surface of the plate are almost unchanged after the discharge of 2 min in Fig. 5. And also from the data of 30, 15 and 2 min, we can use extrapolation to get the positive potential distribution on the plate at 0 min. It is obvious that the potential distribution obtained is very close to that at 2 min and would represent the positive potential at 0 min if the concentration difference near the surface appeared before the discharge. When the positive potential at 0 min is subtracted from the data at different discharge times in Fig. 5, the remainder represents the changed parts in Eq. (1) during this period of the discharge. During the discharge of the plate, the spine voltage drop η_{IR}, is approximately equal to a constant for the same height on the plate. Since the interface between the spine and the active

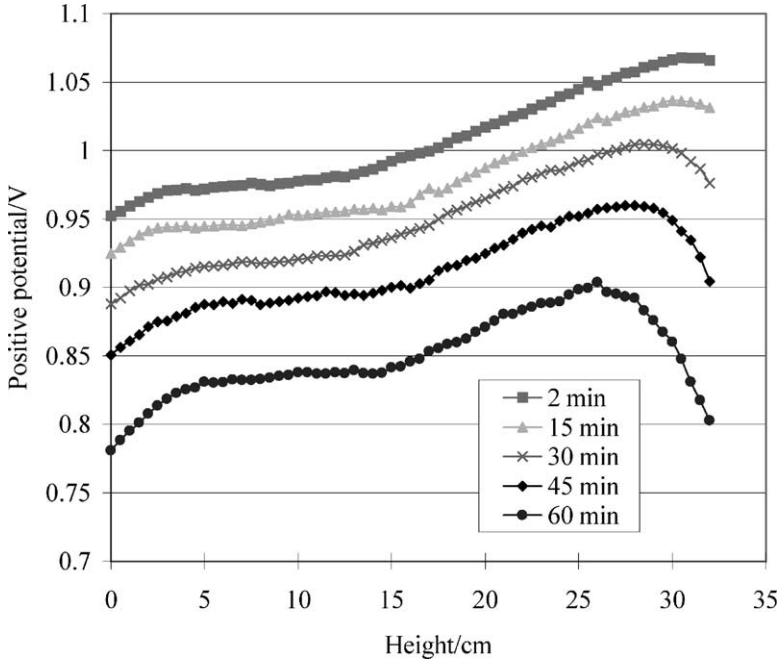

Fig. 5. The positive potential vs. height on the tubular positive plate in channel 2 (near lug) during discharge of 50 A (1 h rate).

mass is formed during the curing, formation and the charge–discharge cycles, its resistance and its voltage drop change a little during one discharge, especially in the early stage of the discharge. Therefore, subtracting the positive potential obtained at 0 min from that at different discharge times gets the changes in the positive overpotential, which reflects the increment of $(\eta_e + \eta_{am})$ in Eq. (1) during the discharge. The resistance increment of the active mass at different parts of the tubular positive plate is shown in Fig. 9. It is found that the resistance increment becomes fast in the later stages of the discharge, especially at the bottom and at the top of the plate. The greatest change in the resistance exists on the top. It can also be seen from Figs. 3 and 5 that at the top of the plate, the potential polarization is the highest, and its current density is the lowest at the end of the discharge. These are closely related to the overcharge and overdischarge at the top of the plate. So great changes take place in the resistance at different parts of the plate. This will lead to great differences of active mass utilization in the later life of the cell.

In order to analyze the change in the positive potential from the bottom to the top of the plate in Fig. 4A, the tubular positive plate was discharged at 50, 30, 16 and 10 A, respectively. It indicates that the potential difference up and down the plate is similar and is proportional to the discharge current.

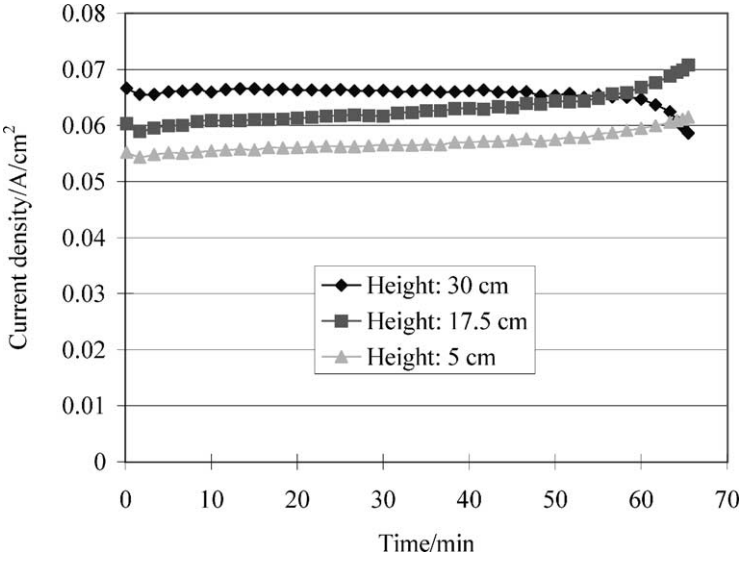

Fig. 6. The evolution of current density at different heights on the tubular positive plate during discharge of 50 A (1 h rate).

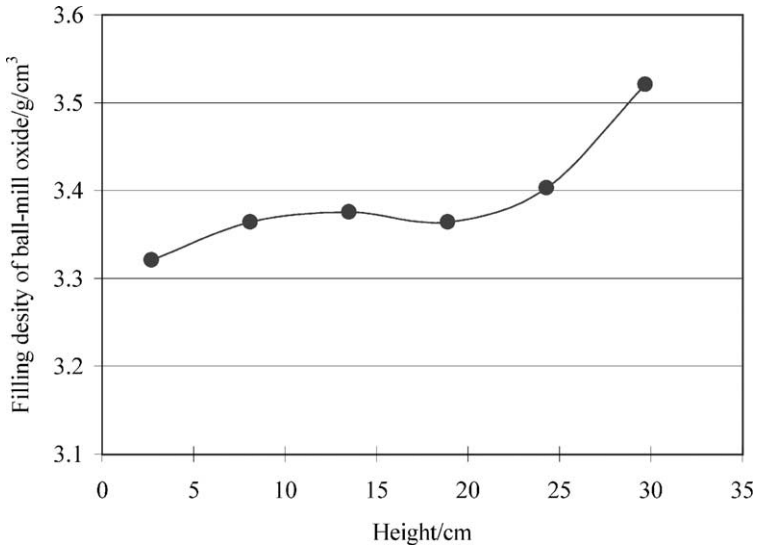

Fig. 7. The distribution of filling density of ball-mill oxide on the tubular positive plate.

When the positive potential tends to stabilize in the initial period of the discharge, the potential drops are about 100, 60 30 and 20 mV in the region from 5 to 30 cm of height, respectively, for the discharge currents of 50, 30, 16 and 10 A. And this always happens when the charge factor of the plate is 1.2. It seems that there is a kind of resistance that varies from the bottom to the top of the plate. In Eq. (1), η_c is the same up and down the plate because the electrolyte is often agitated by gassing. In order to calculate the voltage drop of the spine, η_{IR}, we measured the resistance distribution of the current collectors in Fig. 1A and the results are shown in Fig. 10. It indicates that the resistance increases uniformly with the distance away from the lug. And the maximum resistance from the top to the bottom is only 11–12 mΩ. It is clear that the resistance results in the IR drop. But it is not a major factor in the potential difference up and down the plate in Fig. 5 because the average current of each spine is only 3.33 A for the discharge of 50 A.

In order to deduct the IR drop of the spine, it is assumed that the current distribution is uniform on the plate. Let i denote the current density of the internal surface of the gauntlets, r and y the internal radius and the height of the gauntlet and ρ the specific resistance of the spine. The average specific resistance is 0.347 mΩ cm^{-1}. Therefore, the current, I, and the IR drop, ΔE, of the spine at any height can be expressed by

$$I = \int_0^y 2\pi r i dy = 2\pi r i y \tag{2}$$

$$\Delta E = \int_0^y I\rho dy = \pi r i \rho y^2 \tag{3}$$

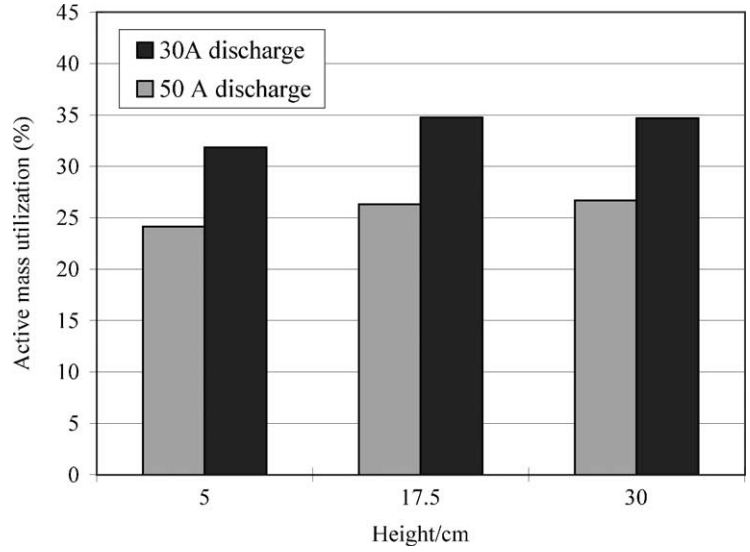

Fig. 8. The active mass utilization ratio at different heights on the tubular positive plate during discharge of 30 and 50 A.

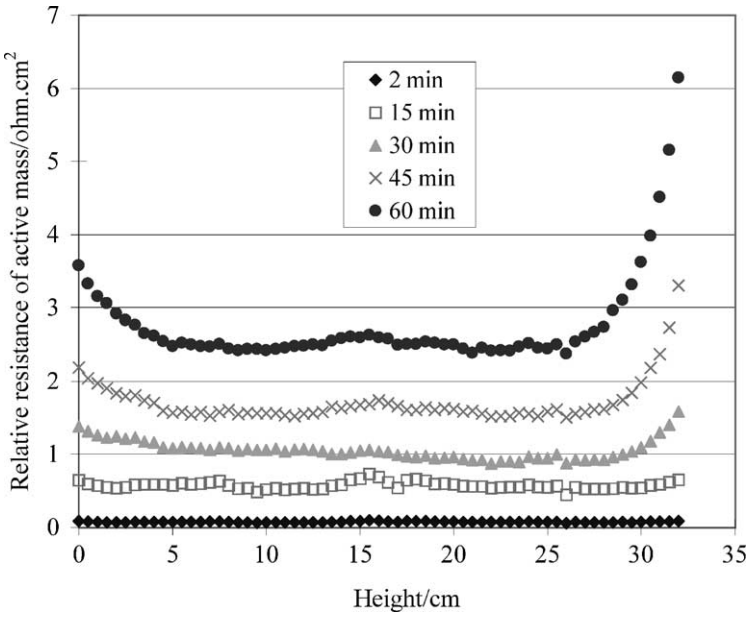

Fig. 9. The relative resistance evolution of active mass on the tubular positive plate during discharge at 50 A (1 h rate).

So the IR drop of the spine increases exponentially with the increase of the height on the plate and the maximum voltage drop only reaches 18.5 mV at the discharge of 50 A. When the current collector is corroded in the manufacture and the cycles of the cell, the specific resistance of the spine rises by about 10%. Thus the maximum voltage drop above is changed to 20.4 mV.

Fig. 11 shows the distribution of the positive potential with and without the spine voltage drop at the discharge of 50 A. In comparison, the current density is also given in Fig. 11. It can also be seen that great changes still take place in the positive potential up and down the plate. It is obvious that the high polarization potential at the bottom of the plate is not caused by the electrochemical reaction because the current density is low in this region. Therefore, it is due to either η_{am} or $\eta_{interface}$ in Eq. (1).

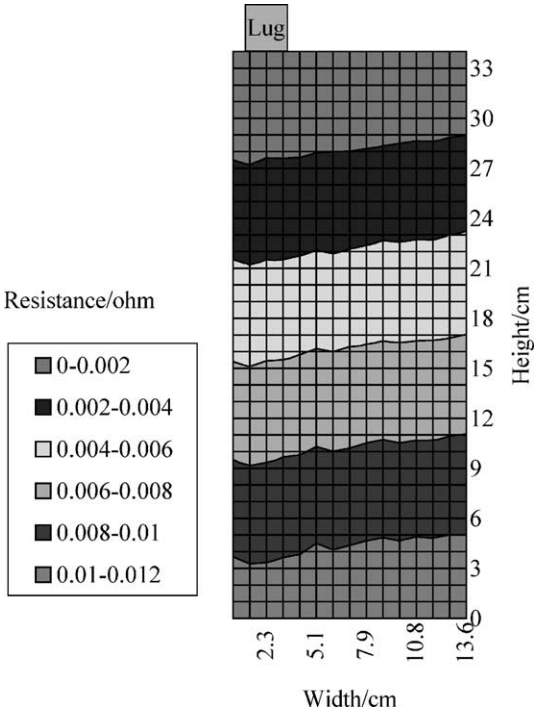

Fig. 10. The resistance distribution of current collectors in Fig. 1A.

In order to study the changes of η_{am} and $\eta_{interface}$, we measured the distribution of the positive potential when the discharged plate is charged at 10 A. The results are shown in Fig. 12. Like Fig. 11, the IR voltage drop of the spine can also be deduced and it makes the charge overpotential become low. So Fig. 12 also shows the distribution of the current and the positive potential without the spine voltage drop. At the charge of 10 A, the maximum IR drop is only 4.1 mV for the spine in Fig. 1A. Actually, the potential polarization up and down the plate is almost the same as that at the discharge of 10 A, except that the polarization direction is different. It is found that the lower the current density, the higher the polarization potential is, especially at the bottom and at the top of the plate. In the entire charge, the voltage drop up and down the plate is almost unchanged and is about 20 mV. The current density in the lower part is always lower than that in the upper part while on the contrary, the higher polarization potential occurs in the lower part. This is different from the behavior of the normal active mass on charge. From the analysis above, η_c, η_{IR} and η_e can not result in the big voltage drop of the plate. It is believed that the voltage drop up and down the tubular positive plate is caused by the interface resistance between the spine and the active mass ($\eta_{interface}$) not by the resistance of the active mass (η_{am}). This is because great changes take place in the resistance of the active mass during charge and discharge. And normally, the higher polarization must lead

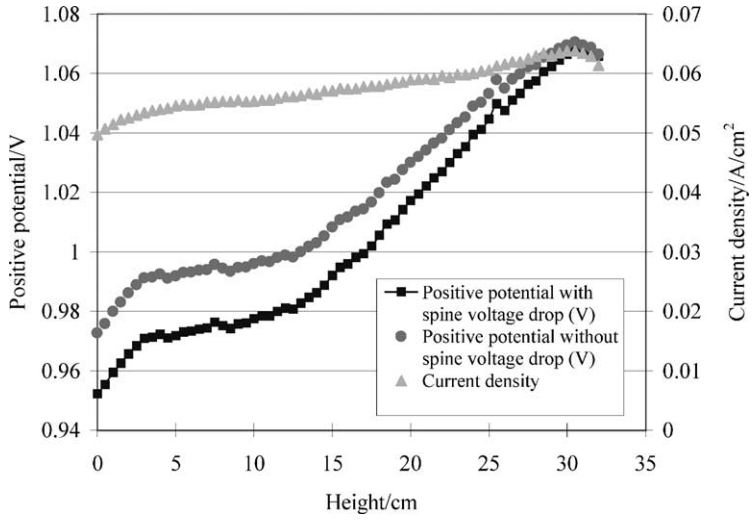

Fig. 11. The distributions of positive potential and current density when the tubular positive plate was discharged at 50 A for 2 min.

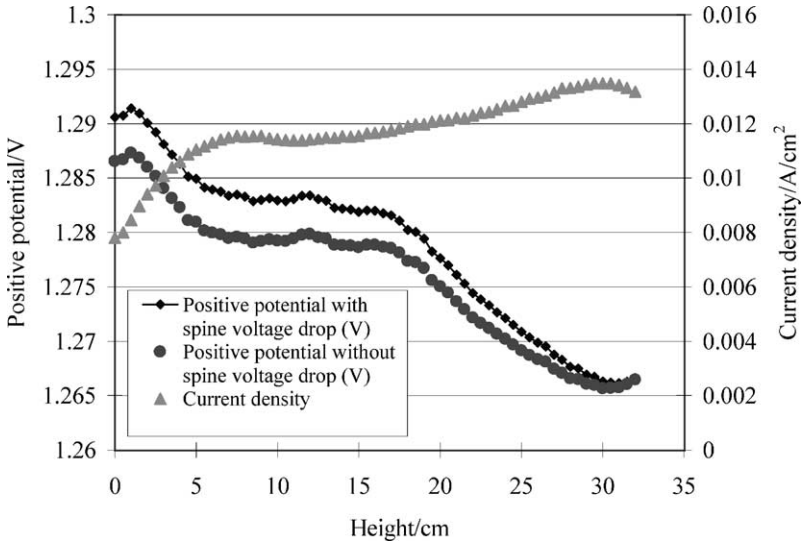

Fig. 12. The distributions of positive potential and current density when the tubular positive plate was charged at 10 A for 0.5 h.

to the higher current density on the active mass, which is contrary to the results in Figs. 11 and 12. Therefore, the interface resistance between the spine and the active mass varies greatly up and down a tall tubular positive plate. And the higher interface resistance appears in the lower part of the plate. This may be related to the insufficient formation and charge in the lower part of a tall plate.

4. Conclusions

The following conclusions can be drawn by measuring the distribution of the potential and current on the tubular positive plate.

(1) On a tall tubular positive plate there exist polarization of the electrochemical reactions, concentration difference, voltage drop of the current collector and resistance of the active mass and interface between the collector and active mass. As a result, great changes take place in the positive potential in different parts of the plate. Usually, the higher polarization occurs lower down the plate. But at the top of the plate, the polarization overpotential increases more rapidly during the discharge. This is because this part of the active mass is often subject to overcharge and overdischarge during the cycling of the batteries.

(2) Since the distribution of the potential is nonuniform, it leads to changes of the current distribution on the tubular positive plate. In the early stages of discharge, the current density in the upper part of the plate is higher than that in the lower part. However, the current on the top of the plate decreases very fast with the discharge. The utilization of the active mass in the upper part is the same as that in the middle due to the denser filling

density of the oxide in the upper part. But it decreases significantly in the lower part of the plate. This is related to the high polarization and low filling density of the oxide.

(3) The resistance distribution on the tubular positive plate is nonuniform. The resistance of the active mass becomes higher and higher during the discharge. And it increases very quickly at the top and at the bottom of the plate. This leads to very high polarization overpotential and low current density in these regions.

(4) Great changes take place in the interface resistance between the active mass and the current collector up and down the plate. The resistance in the lower part is higher than that in the upper part. Consequently, a potential difference of about 100 mV appears up and down the plate, while the IR drop of the spine is only about 20 mV at the discharge of 50 A. The change of the interface resistance and the causes of its formation need further investigation.

References

[1] L. Prout, J. Power Sources 41 (1993) 163.
[2] W.E. Fetzer, J. Power Sources 31 (1990) 255.
[3] J. Kwasnik, H. Krysiak, J. Power Sources 31 (1990) 263.
[4] T. Rogachev, G. Papazov, D. Pavlov, Prog. Batt. Fuel cells 2 (1979) 145.
[5] D.W.H. Lambert, J. Power Sources 28 (1989) 187.
[6] G. Terzaghi, J. Power Sources 73 (1998) 78.
[7] J.M. Stevenson, A.T. Kuhn, J. Power Sources 8 (1982) 385.
[8] A.T. Kuhn, J.M. Stevenson, J. Power Sources 10 (1983) 389.
[9] H.W. Yang, Y.Y. Wang, C.C. Wan, J. Power Sources 15 (1985) 45.
[10] E. Voss, J. Power Sources 7 (1982) 343.
[11] K. Asai, T. Hatanaka, M. Tsubota, K. Yonezu, K. Ando, J. Power Sources 16 (1985) 65.
[12] J. Landfors, D. Simonsson, J. Electrochem. Soc. 139 (1992) 2760, 2768.
[13] R.D. Prengaman, J. Power Sources 78 (1999) 123.
[14] T. Rogachev, D. Pavlov, J. Power Sources 64 (1997) 51.
[15] K.D. Merz, J. Power Sources 73 (1998) 146.
[16] W.G. Sunu, B.W. Burrows, J. Electrochem. Soc. 128 (1981) 1405; W.G. Sunu, B.W. Burrows, J. Electrochem. Soc. 129 (1982) 688; W.G. Sunu, B.W. Burrows, J. Electrochem. Soc. 131 (1984) 1.
[17] L.E. Vaaler, E.W. Brooman, H.A. Fuggiti, J. Appl. Electrochem. 12 (1982) 721.
[18] M. Calabek, K. Micka, P. Baca, P. Krivak, J. Power Sources 85 (2000) 145.
[19] P. Kral, P. Krivak, P. Baca, M. Calabek, K. Micka, J. Power Sources 105 (2002) 35.
[20] Y. Guo, R. Groiss, H. Doering, J. Garche, J. Electrochem. Soc. 146 (1999) 3949.